

## CO<sub>2</sub> Corrosion Behaviors of Tubing and Casing Steels in Simulation Produced Water for Deep Natural Gas Wells

Nan Li<sup>1, a</sup>, Dekui Xu<sup>1, b</sup>, Wenhai Ma<sup>1,2, c</sup>, Pingang Ma<sup>1, d</sup> and Junliang Li<sup>1, e</sup>

<sup>1</sup>Production Engineering & Research Institute of Daqing Oilfield CO. Ltd., Daqing, China

<sup>2</sup>Petroleum & Natural Gas Engineering Institute, Southwest Petroleum University, Chengdu, China

<sup>a</sup>linanln2000@163.com, <sup>b</sup>xudekui@petrochina.com.cn, <sup>c</sup>mawenhai@petrochina.com.cn,

<sup>d</sup>mapingang@petrochina.com.cn, <sup>e</sup>ljlcyy@petrochina.com.cn

**Keywords:** CO<sub>2</sub> Corrosion; Corrosion Products; Tubing and Casing Steels; Deep Natural Gas Wells; Xushen Gasfield

**Abstract.** The influence of temperature and CO<sub>2</sub> partial pressure on tubing and casing steels widely used in Daqing Oilfield including J55, N80 and P110 steels in simulation water for deep natural gas wells with CO<sub>2</sub> corrosion was studied, using autoclave, Scanning Electron Microscope (SEM), Energy Spectrum Analysis (ESA), X-Ray Diffraction (XRD). The results show that the average corrosion rate of the test steel increases rapidly at first as temperature rises until 60°C, then decreases rapidly as temperature continues to rise; the average corrosion rate increases rapidly as CO<sub>2</sub> partial pressure rises until a peak is reached, then tends to be flat as temperature continues to rise; CO<sub>2</sub> corrosion products are mainly FeCO<sub>3</sub> and CaMg(CO<sub>3</sub>)<sub>2</sub>.

### Introduction

CO<sub>2</sub> corrosion and protection are one of the hottest issues all over the world<sup>[1,2]</sup>. Up to now, many studies have been done to obtain some achievements, including mechanism of the corrosion, analysis of influence factors on the corrosion<sup>[3-7]</sup>. However, the corrosion is influenced by many factors, such as medium conditions, working conditions and so on, so that there are many problems different from one another<sup>[8,9]</sup>. Therefore, researchers have studied a lot and many achievements obtained about these problems. As to Daqing, one of the biggest oil and gas fields in the world, there is a large content of CO<sub>2</sub> in natural gas wells in Xushen Gasfield. Since the gasfield was fully developed, the corrosion of downhole tubing and casing have become more and more serious. Through simulation of real working environment in lab experiment, the influence of temperature and CO<sub>2</sub> partial pressure on tubing and casing steels widely used in Daqing Oilfield including J55, N80 and P110 steels in simulation water for deep natural gas wells with CO<sub>2</sub> corrosion was studied and analyzed, using autoclave, Scanning Electron Microscope (SEM), Energy Spectrum Analysis (ESA), X-Ray Diffraction (XRD), the results of which are of certain significance to CO<sub>2</sub> protection on natural gas wells in Xushen Gasfield.

### Experiment

Experimental steels used were J55, N80 and P110, respectively. The size of all test specimens were 50mm×10mm×3mm. The contents of microelements of the steels are shown in Table 1. Experimental medium was simulation water, in terms of the produced water from a gas well in Xushen Gasfield, the pH of which was 6.5. The main contents of the simulation water are shown in Table 2.

Table 1 Percentage contents of microelements of the steels (%)

Steel	C	Si	Mn	P	S	Cr	Mo	Ni	Al	Cu
J55	0.190	0.226	1.544	0.017	0.015	0.049	0.007	0.026	0.052	-
N80	0.240	0.292	1.090	0.015	0.013	0.220	0.018	0.028	0.033	0.001
P110	0.265	0.310	1.320	0.017	0.008	0.958	0.350	0.042	0.062	0.097

Table 2 The main contents of the simulation water

Ion	HCO <sub>3</sub> <sup>-</sup>	Cl <sup>-</sup>	SO <sub>4</sub> <sup>2-</sup>	Ca <sup>2+</sup>	Mg <sup>2+</sup>	Na <sup>+</sup>
Concentration (mg/L)	1735.5	520.7	10.4	120.2	178.3	721.6

The simulation water solution was made up of analytical NaHCO<sub>3</sub>, NaSO<sub>4</sub>, NaCl, CaCl<sub>2</sub>, MgCl<sub>2</sub> and pure water. HCl solution, the mass fraction concentration of which was 0.1%, was used to adjust pH value of the simulation water solution.

Firstly, N<sub>2</sub> gas had been used to inject into the solution for at least 1 hour. Then, static simulation corrosion experiment was done in autoclave, shown in Fig.1. Next, micro-feature of the test specimens after the experiment in autoclave and micro-feature of those blocks after washed and cleaned were observed, using SEM, shown in Fig.2. Then, corrosion products on the surface of the test specimens after the simulation experiment were analyzed and elemental composition of the corrosion products was given, using ESA. Finally, phase composition of the corrosion products was analyzed and chemical compound of the products was given, using XRD, shown in Fig.3.



Fig. 1 Autoclave

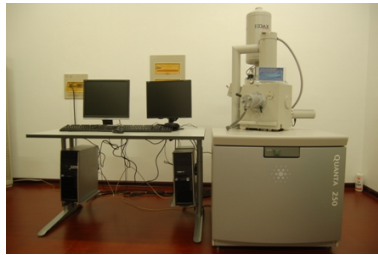


Fig. 2 Scanning Electron Microscope



Fig. 3 X-Ray Diffraction

The experimental period is 72 hours. Parameter combinations of simulation temperature and CO<sub>2</sub> partial pressure are as follows: when CO<sub>2</sub> partial pressure is 5MPa, temperature is 20°C, 40°C, 60°C, 80°C, 100°C; when temperature is 80°C, CO<sub>2</sub> partial pressure is 2MPa, 8MPa, 10MPa, 12MPa.

## Results and Discussion

Under the condition of different temperatures, average corrosion rates of J55, N80, P110 test specimens in simulation produced water for deep natural gas wells were compared, shown in Fig. 4.

Under the condition of different CO<sub>2</sub> partial pressure, average corrosion rates of J55, N80, P110 test specimens in simulation produced water for deep natural gas wells were compared, shown in Fig. 5.

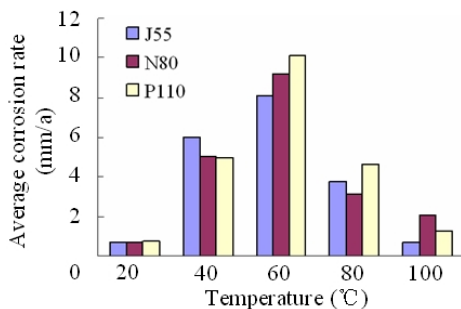


Fig. 4 Comparison of average corrosion rates of the steels under different temperatures

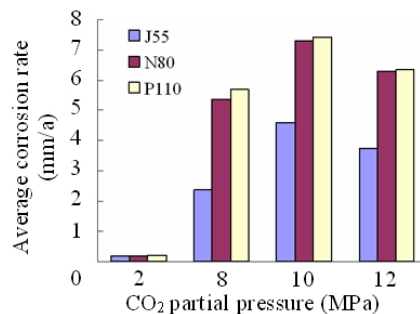


Fig. 5 Comparison of average corrosion rates of the steels under different CO<sub>2</sub> partial pressure

From Fig.4, it can be seen that the influence of temperature on the J55, N80, P110 test specimens is great; the average corrosion rate of the steel starts at 20°C, then increases rapidly at first as temperature rises until 60°C, at which there is a peak, then decreases rapidly as temperature continues to rise.

From Fig.5, it can be seen that the influence of CO<sub>2</sub> partial pressure on the J55, N80, P110 test specimens is great; the average corrosion rate of the steel increases rapidly at first as CO<sub>2</sub> partial pressure rises until 10MPa, at which there is a peak, then tends to be flat as CO<sub>2</sub> partial pressure continues to rise. This phenomenon may be related to solubility of CO<sub>2</sub> in water and protection of corrosion products on the steel. As CO<sub>2</sub> partial pressure increases, concentration of CO<sub>2</sub> in water increases, so that hydrogen depolarization reaction is enhanced, which leads to fast corrosion. But, as CO<sub>2</sub> partial pressure continues to increase, corrosion scale on the surface of the test specimen may protect the steel to some extent, which might counteract what CO<sub>2</sub> partial pressure did to the corrosion of the specimen.

Take J55 steel as an example. When temperature is 80°C and CO<sub>2</sub> partial pressure is 10MPa, its micro-features of pitting corrosion and uniform corrosion in simulation produced water for natural gas wells were obtained, using SEM, shown in Fig. 6.

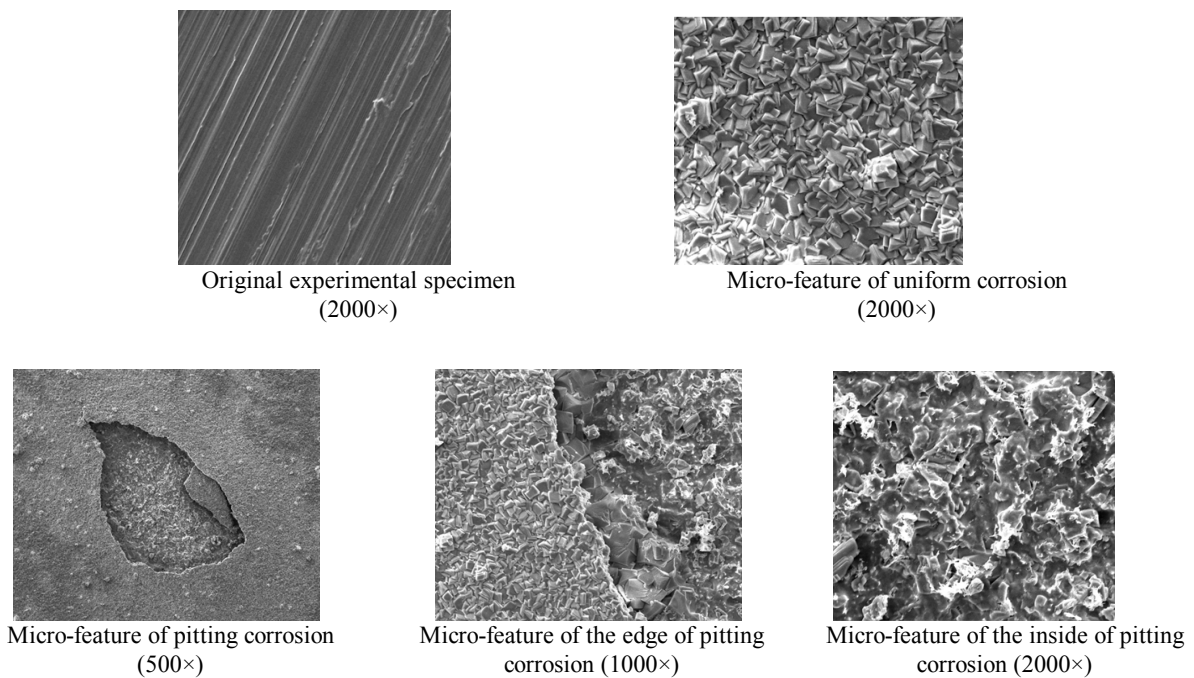


Fig. 6 Micro-feature of uniform and pitting corrosion of J55 steel

From Fig.6, it can be seen that uniform corrosion scale is flat and compact; pitting corrosion scale is loose; pitting corrosion can be aggravated from outside to inside gradually and corrosion perforation is formed eventually; pitting corrosion can be gradually aggravated in side direction, which makes uniform corrosion scale come off, so that new corrosion happens again.

Take P110 steel as an example. When temperature is 80°C and CO<sub>2</sub> partial pressure is 8MPa, results of observation and analysis on corrosion in simulation produced water for natural gas wells were obtained, using ESA, shown in Fig.7, and using XRD, shown in Fig.8, respectively.

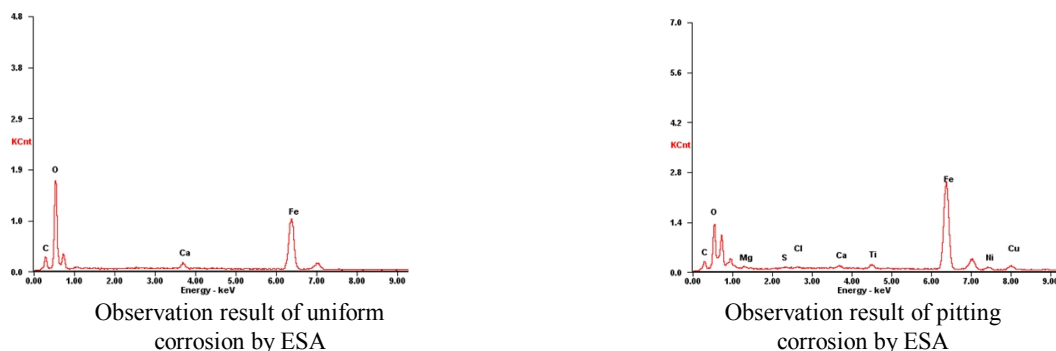


Fig. 7 Observation results of corrosion by ESA

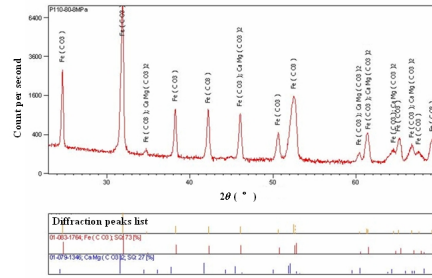


Fig. 8 Analysis results of corrosion by XRD

From Fig.7 and Fig.8, it can be seen corrosion products mainly contain  $\text{FeCO}_3$  and  $\text{CaMg}(\text{CO}_3)_2$ . Through semi-quantitative analysis, the corrosion products mentioned above account for 73% and 27%, respectively. In addition, due to some amount of  $\text{Ca}^{2+}$  and  $\text{Mg}^{2+}$  in the simulation produced water, which may cause chemical reaction with  $\text{CO}_2$  and water,  $\text{CaMg}(\text{CO}_3)_2$  may be generated and adhere to the surface of the test specimen, which leads to formation of cathode. Then, the difference between the anode, metal specimen, and the cathode may become larger and larger, so that corrosion may be aggravated.

### Conclusions

(1) The influence of temperature on J55, N80 and P110 steels in simulation produced water for natural gas wells is great. The average corrosion rates of the steels increase rapidly at first as temperature rises until  $60^\circ\text{C}$ , then decreases rapidly as temperature continues to rise.

(2) The influence of  $\text{CO}_2$  partial pressure on the J55, N80 and P110 steels in simulation produced water for natural gas wells is great. The average corrosion rates of the steels increases rapidly at first as  $\text{CO}_2$  partial pressure rises until 10MPa, at which there is a peak, then tends to be flat as  $\text{CO}_2$  partial pressure continues to rise.

(3)  $\text{CO}_2$  corrosion products mainly contain  $\text{FeCO}_3$  and  $\text{CaMg}(\text{CO}_3)_2$ .

### References

- [1] J. K. Heuer, J. F. Stubbins, An XPS characterization of  $\text{FeCO}_3$  films from  $\text{CO}_2$  corrosion. *J. Corros Sci*, 41(7) (1999): 1231-1243.
- [2] J. Li, Study on the corrosion behavior and mechanism of tubular steel in carbon dioxide environment, Beijing USTB Doctor Dissertation, pp.2-10. (2000). (In Chinese)
- [3] J. M. Zhao, M. G. Gu, Y. Zuo, Influencing factors on corrosion of mild steel in carbon dioxide environment, *J. Beijing Univ. Chem. Tech.*, 32(5) (2005):71 -74. (In Chinese)
- [4] C. F. Li, B. Wang, Y. Zhang, Reseach progress of  $\text{CO}_2$  corrosion in oil/gas field exploitation, *J. Southwest Petroleum Institute*, 26(2) (2004): 42-45. (In Chinese)
- [5] G. F. Lin, Q. Z. Bai, X. W. Zhao, M. S. Zheng, M. X. Lu, Effect of temperature on scales of carbon dioxide corrosion products, *Acta. Petrolei. Sin.*, 25(3) (2004):101 -105. (In Chinese)
- [6] L. P. Wan, Y. F. Meng, F. S. Liang, Carbon dioxide corrosion and its influence factors in oil/gas field exploitation, *J. Total Corrosion and Control*, 17(2) (2003):14 -17. (In Chinese)
- [7] Q. A. Li, Q. Zhang, J. B. Wen, Z. Q. Bai, Prediction and prevention of  $\text{CO}_2$  corrosion of oil tubular goods, *J. Corros. Sci. Prot. Tech*, 16(6) (2004): 381-384. (In Chinese)
- [8] S. L. Wu, Z. D. Cui, F. He, Characterization of the surface film formed from carbon dioxide corrosion on N80 steel, *J. Material Letters*, 58(6) (2004): 1076-1081.
- [9] W. H. Ma, X. H. Pei, F. Gao, Corrosion behaviors of N80 Steel in simulated water from deep gas well containing  $\text{CO}_2$ , *J. Chinese Society for Corrosion and Protection*, 27(1) (2007): 8-12. (In Chinese)